Received: January 12, 2020. Revised: February 27, 2020.

INASS

International Journal of
Intelligent Engineering & Systems

http://www.inass.org/

Robust Nonlinear Controller of the Speed for Double Star Induction Machine in the Presence of a Sensor Fault

Aichetoune Oumar[1]* Rachid Chakib[2] Moussa Labbadi[1] Mohamed Cherkaoui[1]

[1]*Engineering for Smart and Sustainable Systems Research Center, Mohammadia School of Engineers, Mohammed V University in Rabat, Morocco*
[2]*Laboratory of Innovation in Management and Engineering for Enterprise (LIMITE), ISGA, Rabat, Morocco*
* Corresponding author's Email: aichetouna.mahmoud@gmail.com

Abstract: This paper is dedicated to controlling the speed of the double star induction machine (DSIM) by a robust controller. The model of DSIM has been presented by using a vector representation. To control this machine, three robust nonlinear controllers have been used: an active disturbance rejection control (ADRC) regulator is presented in the first place, after a sliding mode control (SMC) is studied in second place, to achieve some performance for the machine, and then followed by the proposed robust controller based on the Backstepping (BSC) technique, this technique is based on the stability of the Lyapunov function. A comparative study between these controllers (ADRC, SMC and BSC) has been presented. The performance of three regulators or three techniques is evaluated under the normal operating condition of the machine and in the presence of one current sensor fault. The simulation of these techniques is presented, the results showed that the proposed controller based on BSC is more robust than that of ADRC Controller and SMC controller.

Keywords: DSIM, Robust controllers, ADRC, SMC, Backstepping, Sensor fault.

1. Introduction

In the fields of industrial applications that require reliability and high power, the multiphase machine occupies an important place, this machine generally has advantages over the three-phase machine such as power segmentation, minimization of torque ripples and rotor losses and also improved reliability [1].

The double star induction machine is the most widely used multiphase machine, it contains six phases in stator subdivided into two windings. It is used in high power applications such as compressors, locomotive traction and in the wind power production system, etc [1, 2].

The control of the DSIM has long been a very broad field of research. One of the first known control is vector control, which is a classical control. The rotor field-oriented control is one of vector control, its principle is to control the DSIM in such a way that the rotor flux is constant on one of the axes of the PARK reference frame [3]. In general, the PI type controller is the one used in this control. The use of the PI regulator for speed control is very sensitive to parameter variation of the machine and the load variation [3]. For this reason, the PI controller has lost its performance, so it is often replaced with a non-linear controller. In addition to this problem, the defect of the currents sensors is also a huge problem that can destroy the performance of the DSIM control system. For this reason, it is very important to develop a controller that can keep a good system performance.

Our aim in this paper is to develop a robust controller based on the backstepping approach which takes into account the parameter variation and the sensor failure. The study consists of regulating the speed of the DSIM by a BSC controller while keeping the regulation of currents and flux by PI controllers, which considered a mixed control. This regulator will be compared to two other nonlinear controllers based on the active disturbance rejection

control (ADRC) technique and the sliding mode control (SMC).

The ADRC is a command introduced by Han [4]. It is a robust non-linear controller, it allows us to estimate and compensate all the disturbances of the system. The main element of this technique is called the ESO which provides the disturbance estimation. The ADRC allows decoupling between the DSIM magnitudes [4]. This control has been applied to the three-phase induction machine in [5] and the doubly- fed induction machine in the reference [6] and has shown its efficiency in these research works. Other references have compared the ADRC controller with the PI controller [6, 7], in this comparison, it has proved that it can replace the PI with good tracking and insensitivity to variation load.

The SMC is a technique for controlling the nonlinear systems and the systems with imprecise models. It is a robust control against the magnitudes variations of the machine and the load variation. This control guarantees the good stability of the machine and fast dynamic response. The SMC has a famous disadvantage called the phenomenon of chattering [8], the chattering causes heat loss and the wear of mechanical systems. This control has demonstrated its performance for the control of the Permanent Magnetic Synchronous Motors [8], doubly fed induction Generator [9].

The Backstepping (BSC) is also a non-linear control method, based on the decomposition of the high-order system into the first-order subsystem. It is a technique that allows in a sequential way to build a Lyapunov function [10]. It is a control that offers good performance in the transient and steady-state even in the presence of parameter variations or load variation. The Backstepping technique has been shown their effectiveness in simulation and experimental research of the control of the three-phase induction machine [10], to the five-phase induction machine [11] and six-phase induction machine [12], it has shown its robustness and efficiency in controlling these types of machines.

This present work is organized as follows: A mathematical model of the machine is presented in section 2. In section 3 a controller based on the ADRC approach is developed. A sliding mode regulator is then presented in section 4. In section 5, a robust controller based on the BSC technique is designed. The system regulation scheme is presented in section 6. In section 7 the performance of the proposed controller, the ADRC and SM controllers are evaluated. Finally, section 8 is reserved for the conclusion.

2. Machine model

The double star induction machine is an electric machine composed of two main elements: the rotor and the stator, the latter consisting of two windings offset by an angle $\alpha = 30°$ [13]. Fig.1 shows the DSIM windings.

The voltages equations of the DSIM in (d, q) axes are expressed by the following system [14]:

$$\begin{cases} V_{ds1} = R_{s1}i_{ds1} + \frac{d}{dt}\psi_{ds1} - \omega_s\psi_{qs1} \\ V_{ds2} = R_{s2}i_{ds2} + \frac{d}{dt}\psi_{ds2} - \omega_s\psi_{qs2} \\ V_{qs1} = R_{s1}i_{qs1} + \frac{d}{dt}\psi_{qs1} + \omega_s\psi_{ds1} \\ V_{qs2} = R_{s2}i_{qs2} + \frac{d}{dt}\psi_{qs2} + \omega_s\psi_{ds2} \\ 0 = R_r i_{dr} + \frac{d}{dt}\psi_{dr} - \omega_{gl}\psi_{qr} \\ 0 = R_r i_{qr} + \frac{d}{dt}\psi_{qr} + \omega_{gl}\psi_{dr} \end{cases} \quad (1)$$

With $\omega_{gl} = \omega_s - \omega_r$

The flux equations [14]:

$$\begin{cases} \psi_{ds1} = L_{s1}i_{ds1} + L_m(i_{ds1} + i_{ds2} + i_{dr}) \\ \psi_{ds2} = L_{s2}i_{ds2} + L_m(i_{ds1} + i_{ds2} + i_{dr}) \\ \psi_{qs1} = L_{s1}i_{qs1} + L_m(i_{qs1} + i_{qs2} + i_{qr}) \\ \psi_{qs2} = L_{s2}i_{qs2} + L_m(i_{qs1} + i_{qs2} + i_{qr}) \\ \psi_{dr} = L_r i_{dr} + L_m(i_{ds1} + i_{ds2} + i_{dr}) \\ \psi_{qr} = L_r i_{qr} + L_m(i_{qs1} + i_{qs2} + i_{qr}) \end{cases} \quad (2)$$

The electromagnetic torque [14]:

$$C_e = P\frac{L_m}{L_m + L_r}(\psi_{dr}(i_{qs1} + i_{qs2}) - \psi_{qr}(i_{ds1} + i_{ds2})) \quad (3)$$

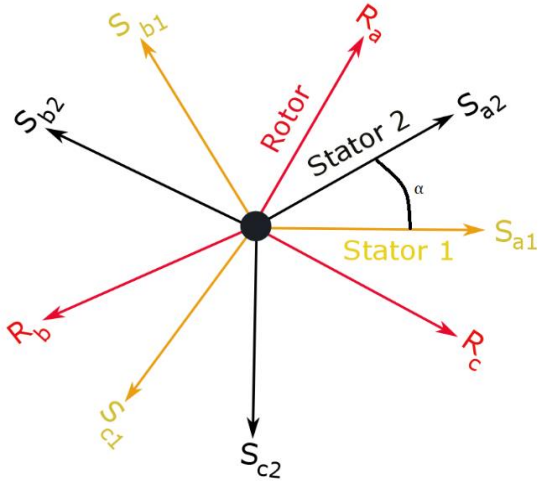

Figure. 1 DSIM windings [9]

The rotor field-oriented control is the one applied in the present study of this paper. The principle of this control is to decouple the torque and the flux in such a way that the flux in the PARK frame is expressed as follows: $\psi_{dr} = \psi_r; \psi_{qr} = 0$ [14].

The electromagnetic torque by applying the principle of vector control becomes:

$$C_e = P\frac{L_m}{L_m+L_r}(\psi_r(i_{qs1} + i_{qs2})) \quad (4)$$

The mechanical equation of the machine is illustrated by Eq. (5).

$$J\frac{d}{dt}\omega_r = C_{em} - C_r - K_f\omega_r \quad (5)$$

By using equations 4 and 5, the speed of the machine is expressed as follows:

$$\frac{d}{dt}\omega_r = \frac{1}{J}\left[P^2\frac{L_m}{L_m+L_r}\psi_r(i_{qs1} + i_{qs2}) - PC_r - K_f\omega_r\right] \quad (6)$$

In this part the model of the system has been presented, in the future section, speed controllers will be presented.

3. ADRC speed regulation

3.1 Principle of the ADRC command

The principle of ADRC command is to estimate all disturbances, whether internal or external to the system and instantly cancel them [15]. An extended state observer (ESO) is the one responsible for estimating disturbances. It treats all unknown system dynamics as a disturbance $f(t)$ [15].

The ADRC principle for a system of *n* order with a single output $y(t)$ is represented by Eq. (7).

$$y^{(n)}(t) = f(t) + b_0U(t) \quad (7)$$

Where $U(t)$ represents the input of the system; $f(t)$ it is the set of disturbances; b_0 is the known parameter of the system. The strategy of the command consists of using the command $U(t)$ to estimate and compensate for $f(t)$.

3.2 ADRC speed regulator

The Fig.2 illustrates the speed regulation diagram. It is clear from the Eq. (5) that the system is first-order so we use a first-order ADRC. The control scheme of the first order and its representation as a state variable is well detailed in the reference [16].

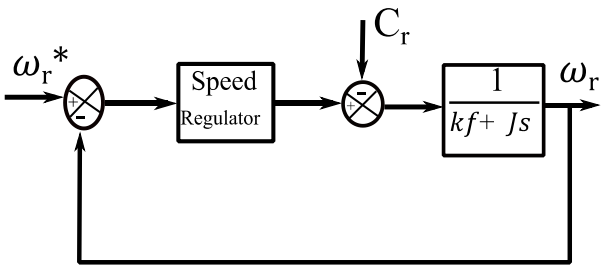

Figure. 2 Speed regulation scheme

We can express Eq. (5) in this form:

$$y^{(1)}(t) = f(t) + b_0U(t) \quad (8)$$

With: $f(t) = \frac{K_f}{J}\omega_r - \frac{C_r}{J} + (\frac{1}{J} - b_0)C_{em}$, $U(t) = C_{em}$ and $b_0 = \frac{1}{J}$.

4. Speed control by SMC

4.1 Principle of the SMC control

It is a control designed to solve the control problems of nonlinear systems. The principle of this control is to define a switching surface and ensure a convergence of the system trajectory to the sliding surface. The sliding mode control is applied in two steps [17, 18-19]. The first step is to define the sliding surface s (t):

$$s(t) = x^* - x \quad (9)$$

Such that x is the state vector of a system and x^* represents, its reference.

The second step consists of determining the control law $u(t)$, this control vector is composed of two terms:

$$u(t) = u_{eq} + u_n \quad (10)$$

u_{eq} : Represents the equivalent control, it is obtained by imposing $\dot{s}(t) = 0$ and u_n : Represents the switching control.

4.2 SMC speed regulator

We must define the sliding surface of the speed:

$$s(t) = \omega_r{}^* - \omega_r \quad (11)$$

The derivative of Eq. (11) is expressed by Eq. (12):

$$\dot{s}(t) = \dot{\omega}_r{}^* - \dot{\omega}_r \quad (12)$$

By replacing Eq. (6) in Eq. (12), we obtain Eq. (13).

$$\dot{s}(\mathrm{t}) = \dot{\omega}_r{}^* - \frac{1}{J}[P^2 \frac{L_m}{L_m + L_r}\psi_r i_{sq}{}^* - PC_r - K_f\omega_r] \quad (13)$$

With: $i_{sq}{}^* = i_{qs1} + i_{qs2}$

We note that $i_{sq}{}^*$ is the control law, it is composed of two terms: an equivalent control term $i_{qs\mathrm{eq}}$ and a switching control term $i_{sq\mathrm{n}}$, illustrated by Eq. (14).

$$i_{sq}{}^* = i_{sq\mathrm{eq}} + i_{sq\mathrm{n}} \quad (14)$$

During steady-state and sliding mode: $s(t)$ =0, $\dot{s}(\mathrm{t}) = 0$ and $i_{sq\mathrm{n}} = 0$, we obtain from Eq. (13) the expression of $i_{sq\mathrm{eq}}$:

$$i_{sq\mathrm{eq}} = \frac{J(L_m+L_r)}{P^2 L_m \psi_r}[\dot{\omega}_r{}^* + \frac{P}{J}C_r + \frac{K_f}{J}\omega_r] \quad (15)$$

From reference [19], $i_{sq\mathrm{n}}$ is calculated by the following equations:

$$i_{sq\mathrm{eq}} = k_\omega \frac{\mathrm{s(t)}}{|\mathrm{s(t)}|+\varepsilon} \quad (16)$$

Where k_ω and ε are positive constants. That stabilizes the closed-loop system and obtained by adjustment.

5. Speed control by BSC

5.1 Principle of the BSC control

The principle of this control is based on the use of the defined positive Lyapunov function, which guarantees an always negative derivative. The Lyapunov calculation is performed after the system has decomposed. The method consists of dividing the system into subsystems of decreasing order. The aim of this strategy is to determine the control of each step while guaranteeing stability [19, 20].

5.2 BSC speed regulator

The purpose of this step is to calculate the difference between the speed ω_r and its reference $\omega_r{}^*$, so the error e is defined by Eq. (17) to referred [19, 20-21].

$$e = \omega_r{}^* - \omega_r \quad (17)$$

The derivative of Eq. (17) is expressed by Eq. (18).

$$\dot{e} = \dot{\omega}_r{}^* - \dot{\omega}_r \quad (18)$$

By replacing in Eq. (18) the derivative of speed represented by (Eq. (6)), we obtain Eq. (19).

$$\dot{e} = \dot{\omega}_r{}^* - \frac{1}{J}[P^2 \frac{L_m}{L_m+L_r}\psi_r(i_{qs1} + i_{qs2}) - PC_r - K_f\omega_r] \quad (19)$$

The Lyapunov function of the speed error is represented by Eq. (20).

$$V = \frac{e^2}{2} \quad (20)$$

The derivative of Eq. (20) is expressed by Eq. (21).

$$\dot{V} = e\dot{e} \quad (21)$$

To get a negative derivative of the function of Lyapunov, it is necessary to choose: $\dot{e} = -G.e$, where G is a positive gain, which implies that the derivative of the function of Lyapunov is strictly negative, therefore the conditions of stability are checked.

From Eq. (19) we get this equality:

$$-G.e = \dot{\omega}_r{}^* - \frac{1}{J}[P^2 \frac{L_m}{L_m + L_r}\psi_r(i_{qs1} + i_{qs2}) - PC_r - K_f\omega_r] \quad (22)$$

From Eq. (22), we get Eq. (23).

$$i_{sq}{}^* = \frac{J(L_m+L_r)}{P^2 L_m \psi_r}[\dot{\omega}_r{}^* + \frac{P}{J}C_r + \frac{K_f}{J}\omega_r + G.e] \quad (23)$$

With: $i_{sq}{}^* = i_{qs1} + i_{qs2}$

The third method presented in this part is the backstepping controller, this method guarantees the stability of the DSIM according to the Lyapunov theory.

6. System regulation scheme

The DSIM control block diagram is illustrated in fig. 3. This scheme consists of a double star induction machine powered by two voltage inverters controlled by the PWM technique, the control scheme is based on vector control. The current and the flux regulation is provided by PI regulators, the speed regulation is provided by an ADRC regulator in a first test, a SMC regulator in the second test and a BSC regulator in the third test. The amplitude of the rotor flux and its phase shift is calculated by an estimator. The flux estimator is based on the following mathematical equation [22]:

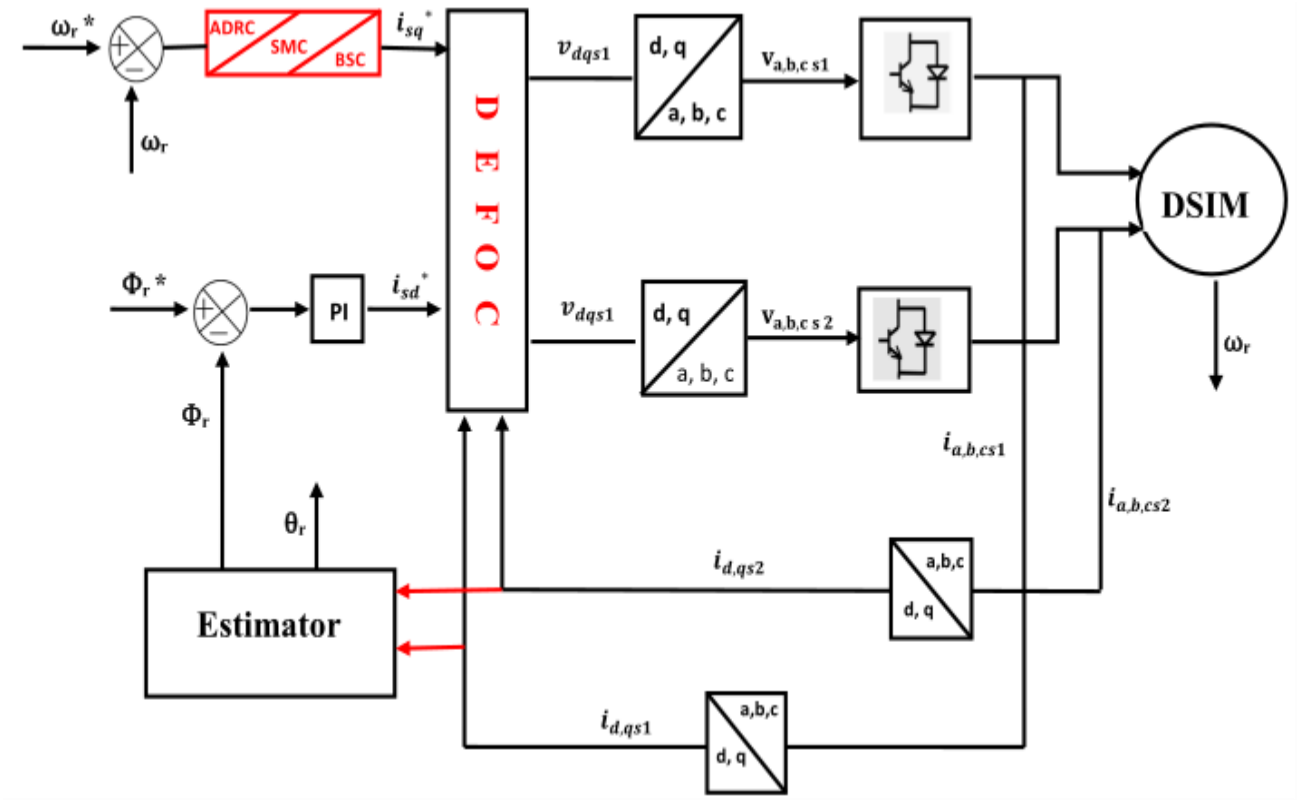

Figure. 3 Control of DSIM

$$\psi_r = \frac{L_m}{1+Tr.s}\,(i_{ds1} + i_{ds2}) \qquad (24)$$

With $Tr = \frac{L_r+L_m}{R_r}$

Its phase shift is calculated by Eq. (25).

$$\theta_s = \int (\frac{R_r L_m}{L_r+L_m}\frac{(i_{qs1}+i_{qs2})}{\psi_r} + \omega_r)dt \qquad (25)$$

7. Comparison between ADRC & SMC and BSC

To verify the robustness of the proposed controller based on the Backstepping technique, we compare it with an ADRC controller and SMC controller. To compare the three controllers, one current sensor fault was introduced on each control structure. Two simulation tests are presented in this section. The first consists of operating the DSIM in a normal state without any fault, the second consists of creating a sensor fault in phase a.

The DSIM studied in this simulation is powered by two voltage inverters controlled by the PWM technique. The parameters of the machine are given in an appendix. In both simulation tests, The DSIM runs empty until we introduce a load torque of 15 N.m at the instant t = 1s also the reference speed is fixed at 100 rad / s. At the level of the second test, we introduce the defect at time t = 3s, where we multiply the amplitude of the measured signal of i_{sa1} by a gain of 1.6 (offset defect) for the first time and in the second time by 0.4 (gain defect).

7.1 Tracking test: Healthy operating

Figs. 4 - 6 illustrate the curves of the speed, the torque and the stator currents of phase a respectively of three controllers. It can be seen from fig. 4 that the torque of each approach follows its desired values. We note that the dynamics response of the torque of the BSC is the fastest.

At the level of the speed curves presented in fig. 5, it is noted that the speed tracks its reference in each control techniques but the response time for the ADRC command is 0.3 s greater than the response time of the SMC that is equal to 0.12 s and BSC command which is equal to 0.1s. It can be observed, in the introduction of the load torque, that the drop in speed amplitude of ADRC control (93 rad/s) is greater than the drop of SMC control (96.8 rad/s) which is also greater than the drop of BSC (99 rad/s). Concerning the curves of the stator currents of each control illustrated by fig. 6 and by zooming on the three curves (fig. 7), it is noted that the current i_{sa1} of all techniques are perfectly sinusoidal without ripples.

From these results, we conclude that the BSC command presents a better performance compared to the ADRC and the SMC.

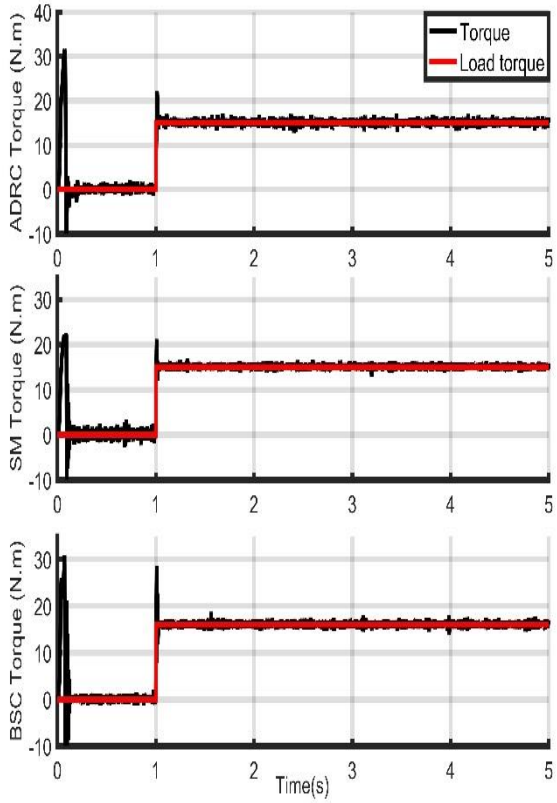

Figure. 4 Electromagnetic Torque

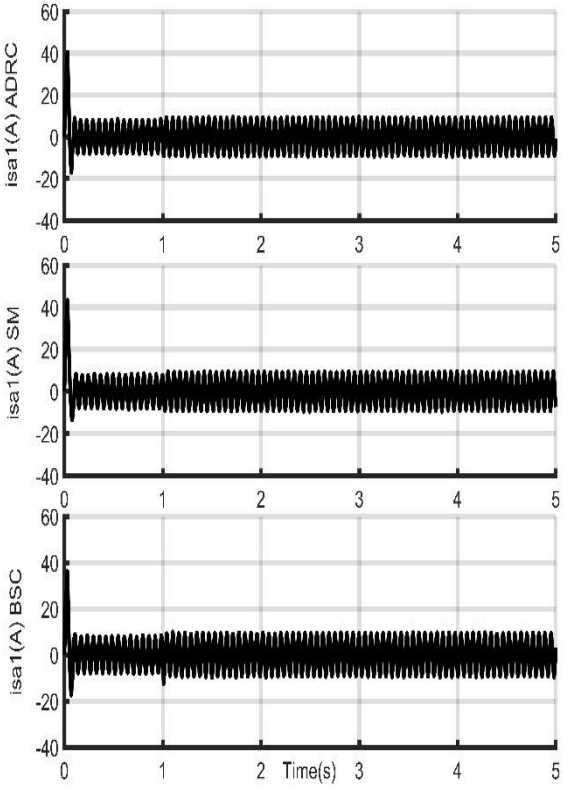

Figure. 6 Stator current i_{sa1} (ADRC & SMC &BSC)

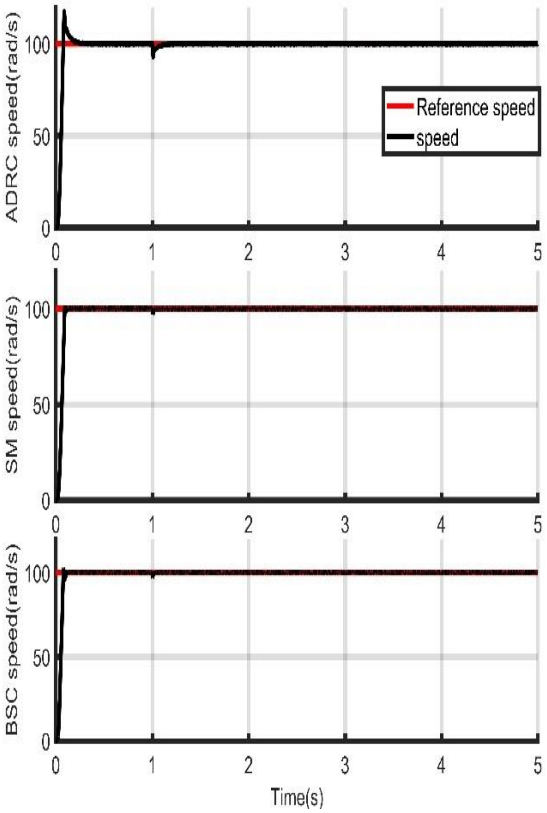

Figure .5 Speed and speed reference (ADRC & SM & BSC)

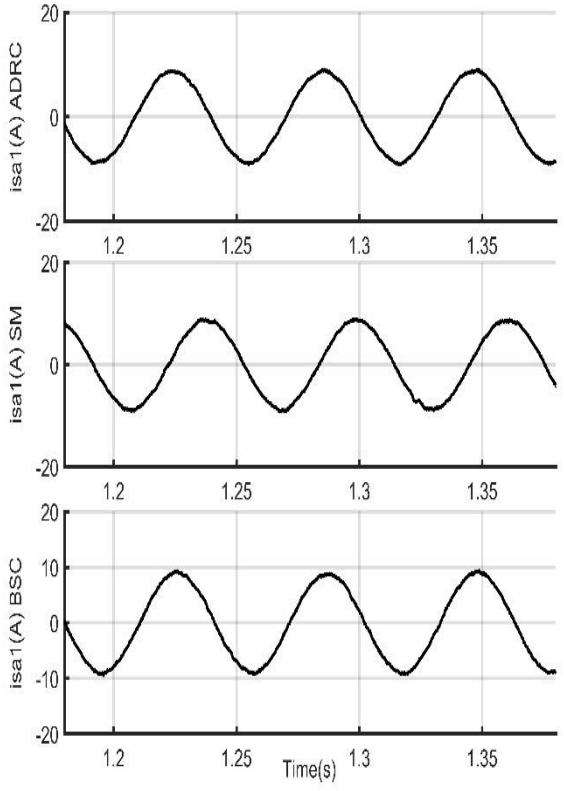

Figure .7 Zoom of Stator current i_{sa1} (ADRC & SMC &BSC)

7.2 Current sensor fault test

In this part we will present two cases of current sensor failure: the first one consists of multiplying the amplitude of the current of phase a, of stator 1 by a gain of 1.6 and the second one consists of multiplying the amplitude of phase a by 0.4.

A. Gain equal to 1.6

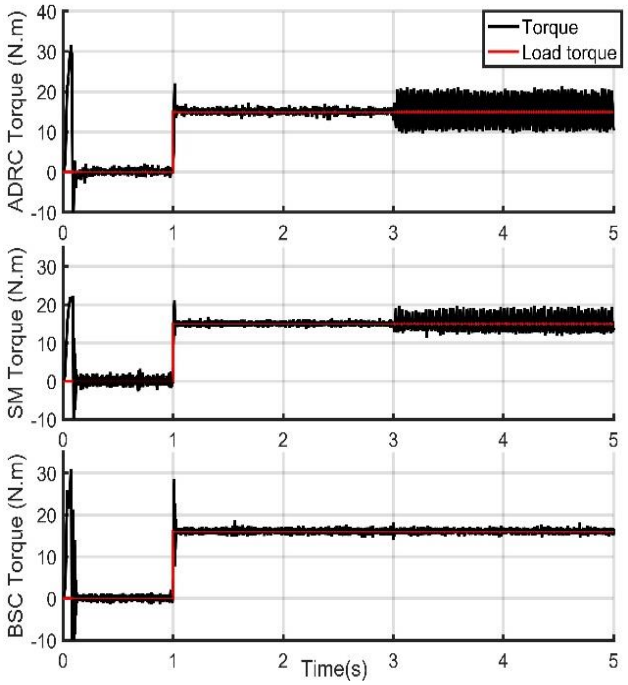

Figure 8. Electromagnetic Torque when current sensor occurred in phase a (gain of 1.6)

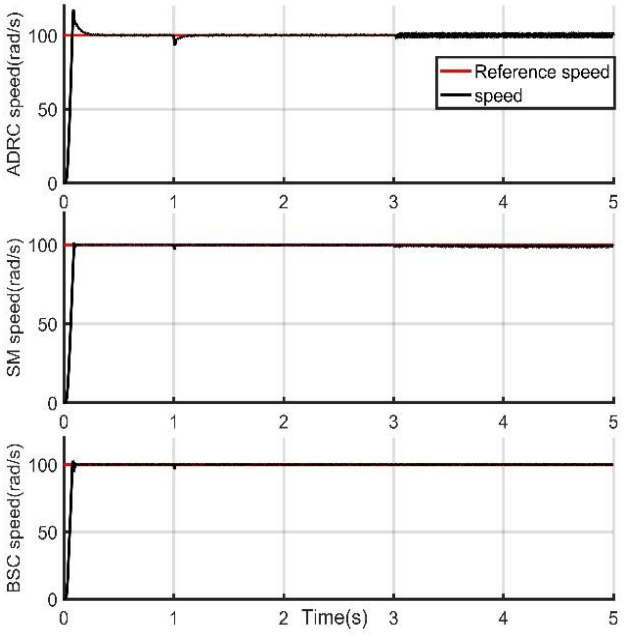

Figure 9. Speed when current sensor occurred in phase a (gain of 1.6)

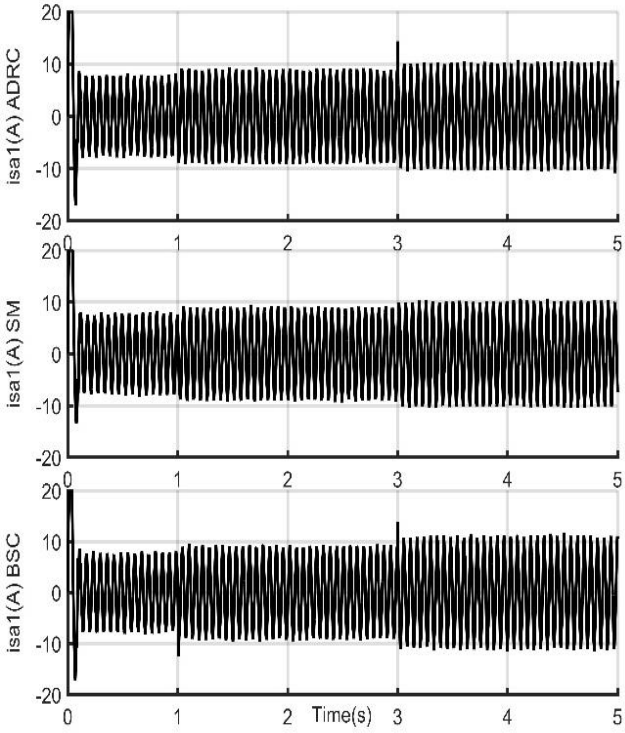

Figure 10. Stator current i_{sa1} when current sensor occurred in phase a (gain of 1.6)

B. Gain equal to 0.4

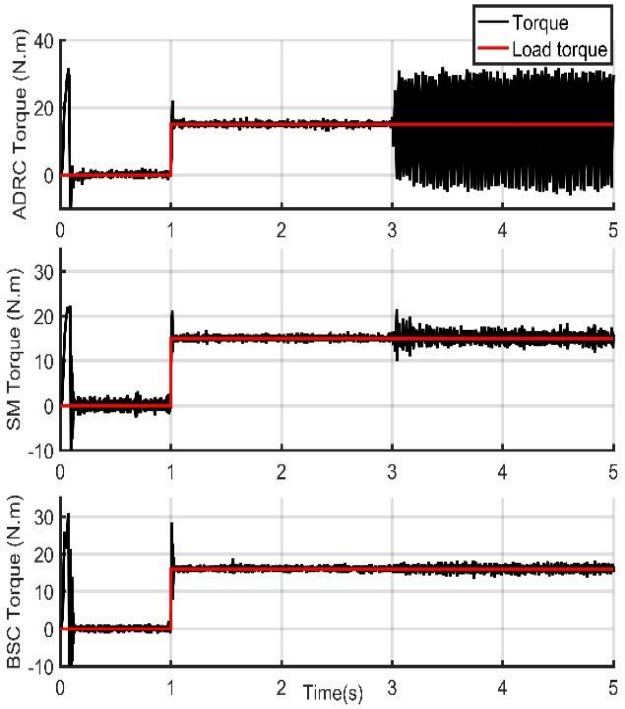

Figure 11. Electromagnetic Torque when current sensor occurred in phase a (gain of 0.4)

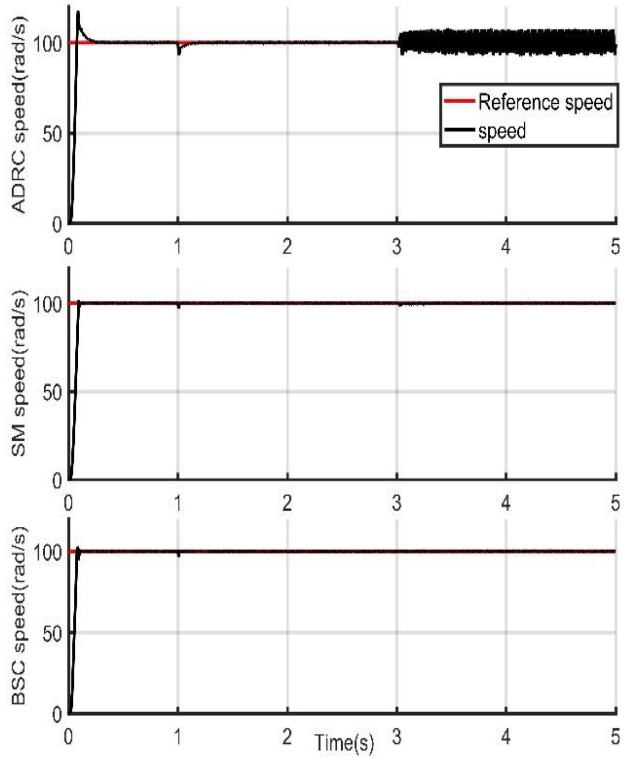

Figure 12. Speed when current sensor occurred in phase a (gain of 0.4)

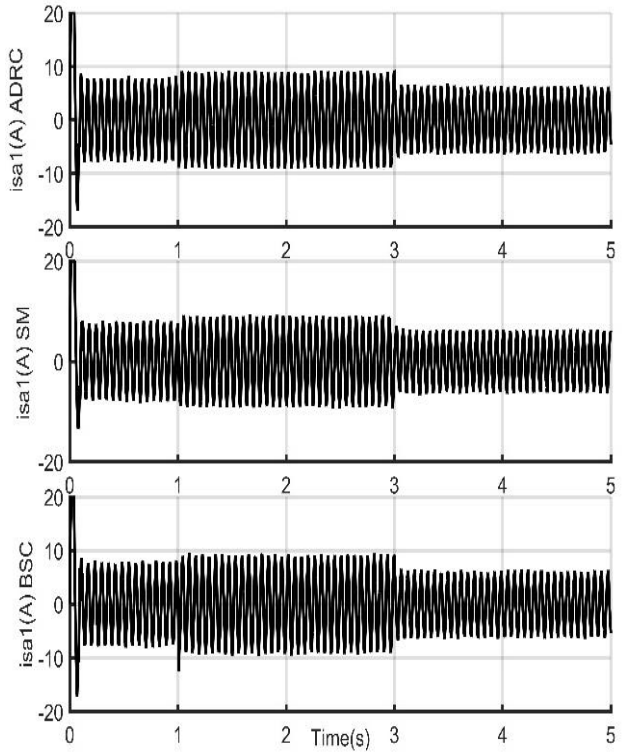

Figure 13. Stator current i_{sa1} when current sensor occurred in phase a (gain of 0.4)

Figs. 8 - 13 illustrate the operation of the DSIM under failure of a current sensor (phase a) at t=3s. We can see from the fig.8 and fig.11 that the electromagnetic torque of the BSC always follows its reference even when a fault is present, unlike the ADRC torque and SMC torque where we can see the presence of strong ripples and oscillations after the occurrence of a fault.

The speed curves presented in the fig. 9 (gain equal to 1.6) of three controllers follow their reference even after the presence of a fault but with small oscillations of the ADRC speed around its reference and negligible oscillations of SMC curve around its reference.

From the speed curve presented in fig. 12 (gain equal to 0.4), we can see that the speed of the BSC and SMC always follow their references even when a fault is present but the ADRC speed curve presented an important oscillation after the fault has occurred.

The existence of a fault does not affect the current of BSC, i_{sa1} curve shown in fig.10 and fig. 13. It's still sinusoidal. The ADRC current and the SMC current are less sinusoidal than the BSC, there are not perfectly smooth.

It is clear that the BSC control is very robust in the presence of a current sensor it ensures the best performance.

8. Conclusion

The purpose of this paper is to design a robust speed controller that takes into account the presence of a current sensor fault. This controller is based on the BSC technique. Other robust controllers based on the ADRC approach and SMC are presented in this paper. Each controller is implemented and simulated in Matlab Simulink. The efficiency of the proposed BSC regulator is compared to the ADRC regulator and SMC regulator.

The results of the tracking test (Healthy operating) and the current sensor fault test have shown that the BSC command is a fast command with more precision and robustness against the default of one current sensor. The ADRC and SMC control, in turn, have shown that there are unable to control the machine in default case and have a slower response time than the BSC.

The contribution of this paper is the design of a BSC controller that takes into account a sensor fault. Using the ADRC technique for controlling the DSIM speed and make for the first time a comparison between the BSC, ADRC and SMC.

Appendix

Notations

V_{ds1}, V_{ds2} , V_{qs1}, V_{qs2}	Voltages of Stator 1 and 2 in d-q axis respectively.

i_{ds1}, i_{ds2} , i_{qs1}, i_{qs2}	Current of Stator 1 and 2 in d-q axis respectively.
ψ_{ds1}, ψ_{ds2} ,ψ_{qs1}, ψ_{qs2}	Flux of Stator 1 and 2 in d-q axis respectively.
ψ_{dr}, ψ_{qr}	Flux of rotor in d-q axis.
C_r	Load torque
R_{S1}, R_{S2}	Stator Resistances (stator 1 and 2)
R_r	Rotor Resistance
L_{S1}, L_{S2}	Stator self-inductances (stator 1, 2)
L_r	Rotor self-inductance
L_m	Cyclic mutual inductance between stator 1, stator 2 and rotor.
N_s,N_r	The number of coil per stator phase, rotor phase respectively
ω_s	Stator speed in rad/s
ω_r	Rotor speed in rad/s
g	Slip
P	Number of pole pairs

Parameters of the DSIM:

Rated power 4.5 KW
Number of pole pairs P = 2
Stator and rotor resistors:
R_{S1}= R_{S2} =0.86Ω, R_r =0.36Ω.
Stator and rotor inductances:
L_{S1}= L_{S2} =0.184H, L_r =0.0246H.
Mutual inductance: L_m =0.0537H
Moment of inertia: J = 0.025 kg.m2
Coefficient of friction: K_f = 0.001Nms/rad

References

[1] L. Bentouhami, R. Abdessemed, Y.Bendjeddou, and E. Merabet, "Neuro-Fuzzy Control of a Dual Star Induction Machine", Journal *of Electrical Engineering*, Vol. 16, No. 4, pp. 1-8, 2016.

[2] R. Sadouni, A.Meroufel, and S. Djriou, "Study and Simulation of Direct Torque Control (DTC) for a Six Phase Induction Machine (SPIM)", *International Journal of Energy*, Vol. 7, No. 2, pp. 31-37, 2013.

[3] E. Merabet, R. Abdessemed, H. Amimeur, and F.Hamoudi, "Field Oriented Control of a Dual Star Induction Machine Using Fuzzy Regulators", In: *Proc. of CIP*, pp. 1-7, 2007.

[4] Y. Huang and W. Xue, "Active disturbance rejection control: methodology and theoretical analysis", *ISA Transactions*, Vol. 53, No. 4, pp. 963-976, 2014.

[5] H. Chalawane, A. Essadki, T. Nasser, and M. Arbaoui, "A New Robust Control Based on Active Disturbance Rejection Controller for Speed Sensorless Induction Motor", In: *Proc. of the* 3rd *International Conference on Electrical and Information Technologies*, pp.1-6, 2017.

[6] M. Arbaoui, A. Essadki, T. Nasser, and H. Chalawane, "Comparative Analysis of ADRC & PI Controllers Used in Wind Turbine System Driving a DFIG", *International Journal of Renewable Energy Research*, Vol.7, No.4, 2017.

[7] H. Laghridat, A. Essadki, and T. Nasser, "Comparative Analysis between PI and Linear-ADRC Control of a Grid Connected Variable Speed Wind Energy Conversion System Based on a Squirrel Cage Induction Generator", *Hindawi Mathematical Problems in Engineering*, Vol. 2019, pp.1-16, 2019.

[8] S. Dandan, D.Yugnag, and Z. Chengning, "Sliding Mode Controller for Permanent Magnetic Synchronous Motors", *Energy Procedia*, Vol.105, pp.2641-2646, 2017.

[9] D. Kairous and R. Wamkeue, "Sliding-mode control approach for direct power control of WECS based DFIG", In: *Proc. of EEEIC*, pp.1-4, 2011,

[10] M. Fateh and R. Abdellatif, "Comparative study of integral and classical backstepping controllers in IFOC of induction motor fed by voltage source inverter", *International journal of Hydrogen Energy*, Vol.42, pp.17953-17964, 2017.

[11] H. Echeikh, R. Trabelsi, A. Iqbal, N. Bianchi, and, M. F. Mimouni, "Non-linear backstepping control of five-phase IM drive at low speed conditions-experimental implementation", *ISA Transactions*, Vol. 65, pp.244-253, 2016.

[12] N. Layadi, S. Zeghlache, T. Benslimane, and F. Berrabah, "Comparative Analysis between the Rotor Flux Oriented Control and Backstepping Control of a Double Star Induction Machine (DSIM) under Open-Phase Fault", *AMSE Journals AMSE IIETA*, Vol. 72, No.4, pp. 292-311,2017.

[13] F. Hamidia, A. Abbadi, and M.S. Boucheri, "Direct torque controlled Dual Star Induction Motors (in open and closed loop)", In: *Proc. of the 4th IEEE International Conference on Electrical Engineering*, pp. 1-6, 2015.

[14] M. H. Lazreg and A. Bentaallah, "Speed sensorless vector control of double star induction machine using reduced order observer and MRAS estimator", In: *Proc. of the 5th International Conference on Electrical Engineering – Boumerdes (ICEE-B)*, pp. 1-6, 2017.

[15] J. Han, "From PID to Active Disturbance Rejection Control", *IEEE Transactions on Industrial Electronics*, Vol. 56, No. 3, 2009.
[16] R. Chakib, M. Cherkaoui, and A.Essadki, "Stator Flux Control by Active Disturbance Rejection Control for DFIG Wind Turbine during Voltage Dip", *International Journal of Circuits, Systems and Signal Processing*, Vol. 9, pp.281-288, 2015.
[17] H. Amimeur, D. Aouzellag, R. Abdessemed, and K.Ghedamsi, "Sliding mode control of a dual-stator induction generator for wind energy conversion systems", *International Journal of Electrical Power & Energy Systems*, Vol.42, No.1, pp.60-70, 2012.
[18] O. Moussa, R. Abdessemed, S. Benaggoune, and H. Benguesmia, "Sliding Mode Control of a Grid-Connected Brushless Doubly Fed Induction Generator", *European Journal of Electrical Engineering*, Vol. 21, No. 5, pp. 421-430, 2019.
[19] N. Layadi, S. Zeghlache, F. Berrabah, L. Bentouhami, "Comparative Study between Sliding Mode Control and Backstepping Control for Double Star Induction Machine (DSIM) under Current Sensor Faults", *International Journal of Information Technology and Electrical Engineering*, Vol. 6, pp. 67-77, 2017.
[20] T. Roubache, S. Chaouch, and M. Naït-Saïd, "Backstepping design for fault detection and FTC of an induction motor drives-based EVs", *Automatika*, Vol.57, pp. 736–748, 2017.
[21] N. Layadi, S. Zeghlache, A. Djerioui, A. Houari, M. Benkhoris, and F. Berrabah, "Integral Backstepping Control for Double Star Induction Machine (DSIM)", In: *Proc. of CISTEM'18*, pp.1-6, 2018.
[22] M. Slimenea and M. Khlifib, "Modeling and digital field-oriented control for double star induction motor drive", *International Journal of Applied Electromagnetics and Mechanics*, Vol. 56, No. 4, pp. 511–520, 2018.